ORIGINAL ARTICLE

Eur. J. Anat. 23 (3): 167-175 (2019)

Surgical landmarks of the glossopharyngeal nerve

Seth Morrill[1], Vikas Mehta[2], Jonathan J. Wisco[3,4,5], Elizabeth Disbrow[6], Mitzi C. Glover[7]

*[1]Department of Cellular Biology and Anatomy, Louisiana State University – Shreveport, Shreveport, Louisiana, USA, [2]Department of Otolaryngology/Head and Neck Surgery, Louisiana State University Health-Shreveport, Shreveport, Louisiana, USA, [3]Department of Physiology and Developmental Biology, Neuroscience Center, Brigham Young University, Provo, UT 84602, [4]Department of Neurobiology and Anatomy, University of Utah Medical School, Salt Lake City, UT 84132, *Department of Anatomy and Neurobiology, Boston University School of Medicine, Boston, MA 02118 [6]Department of Pharmacology, Toxicology, and Neuroscience, Louisiana State University – Shreveport, Shreveport, Louisiana, USA, [7]Department of Cell Biology and Anatomy, Louisiana State University – New Orleans, New Orleans, Louisiana, USA*

SUMMARY

Damage to the glossopharyngeal nerve can occur as a result of various Head and Neck surgeries. Associated with this damage are assorted side effects, such as dysphagia, xerostomia, and loss of taste. This study serves to create probabilistic maps of the glossopharyngeal nerve using quantitative data, and to identify different landmarks in order to locate the nerve. Eleven cadaveric heads were bilaterally dissected to expose and measure the glossopharyngeal nerve. The mastoid process is a more reliable marker for the location of the glossopharyngeal nerve as it stretches through the lateral neck. Additionally, distance landmark measurements from the nerve leaving the jugular foramen to it entering the pharyngeal space are offered. Furthermore, statistical probability equations for nerve location have been created. Measurements and models created by this study will aid in pre-operative identification of glossopharyngeal nerve landmarks that will lead to an increase in quality of life in Head and Neck surgery patients.

Key words: Glossopharyngeal nerve – Head and neck surgery – CN IX

Corresponding author: Jonathan J. Wisco, Ph.D. Boston University School of Medicine, Department of Anatomy and Neurobiology, Laboratory for Translational Anatomy of Degenerative Diseases and Developmental Disorders (TAD4), 72 E Concord St, L-1004, Boston, MA 02118, USA. Phone: 617-358-2002; Mobile: 310-746-6647.
E-mail: jjwisco@bu.edu

INTRODUCTION

The American Academy of Otolaryngology-Head and Neck Surgery defines head and neck cancers as those including the tongue, pharynx, larynx, nasal cavity, paranasal sinuses, thyroid gland, salivary gland, lips, and oral cavity, and states that these cancers account for six percent of all cancer cases in the U.S. Most of these are squamous cell carcinomas, and generally more than half of these are already in advanced stages at the time of diagnosis (Sanderson and Ironside, 2002; Surgery AAOO-Han, 2014).

Head and neck cancer treatments have advanced from the primitive beginnings of radiation as a monotherapy, to the rise of surgical treatment as a primary remedy, to the current therapies, consisting of combinations of surgery, radiation, and chemotherapy (Cognetti et al., 2008). New approaches to surgical excision of head and neck cancers, such as transoral robotics surgery (TORS), create the possibility of less invasive operations requiring less hospitalization time and greater accuracy in the surgical procedure (Boudreaux et al., 2009). In spite of new and advanced treatment options, several side effects may occur, including dryness of the mouth (xerostomia), difficulty in swallowing (dysphagia), tooth decay, loss or change of taste, and decreased appetite (Oncology Asoc., 2014; Institute NC, 2013). All of these side effects can be traced back to diminished nervous control to the pharyngeal region likely caused by damage to the pharyngeal plexus, composed of the vagus nerve, glos-

Submitted: 16 October, 2017. *Accepted:* 14 March, 2019.

sopharyngeal nerve, and sympathetic nerves (Kitagawa et al., 2002; Sakamoto, 2009). With a weakened ability to swallow, there is an increased likelihood of residual material falling into the airway, leading to aspiration. Therefore, dysphagia can lead to a diminished quality of life of individuals in the form of malnutrition, dehydration, and aspiration pneumonia (Pikus et al., 2003; Nguyen et al., 2005).

The glossopharyngeal nerve (GPN) is the ninth cranial nerve, being formed by both motor and sensory fibers from different areas, such as the parotid salivary gland, the stylopharyngeus muscle (SPM), the carotid sinus, the body, etc. The nerve exits the soft tissue of the lateral medulla and travels anterolaterally to exit the cranium via the jugular foramen. The innervation of the SPM occurs via 2 nerve branches exiting the main nerve body.

Human anatomy, while not always 100% consistent, does follow the same general layout. Many of the essential anatomical structures, like the vasculature and bones, are easily visualized with imaging technologies such as computed tomography (CT) or magnetic resonance imaging (MRI). Other significant structures, like the facial nerve, have been comprehensively mapped out (Pereira et al., 2004; Pather and Osman, 2006; Greyling et al., 2007). No such tools or maps are presently available for the glossopharyngeal nerve, despite the negative side effects that ensue from damage to this nerve. The purpose of this study was to create a map of the GPN utilizing quantitative data and modeling that will aid surgeons in their work to preserve the nerve and to increase quality of life for individuals with head and neck cancers.

MATERIALS AND METHODS

Heads were received from the LSU Health Shreveport Willed Body Program with ages ranging from 69 to 92, including six males and five females (n=11). Cadaver heads were briefly inspected and judged to be normal or not based upon gross malformations. Cadavers with head or cranial procedures, or obvious malformations, were excluded from the study. Embalming was per-

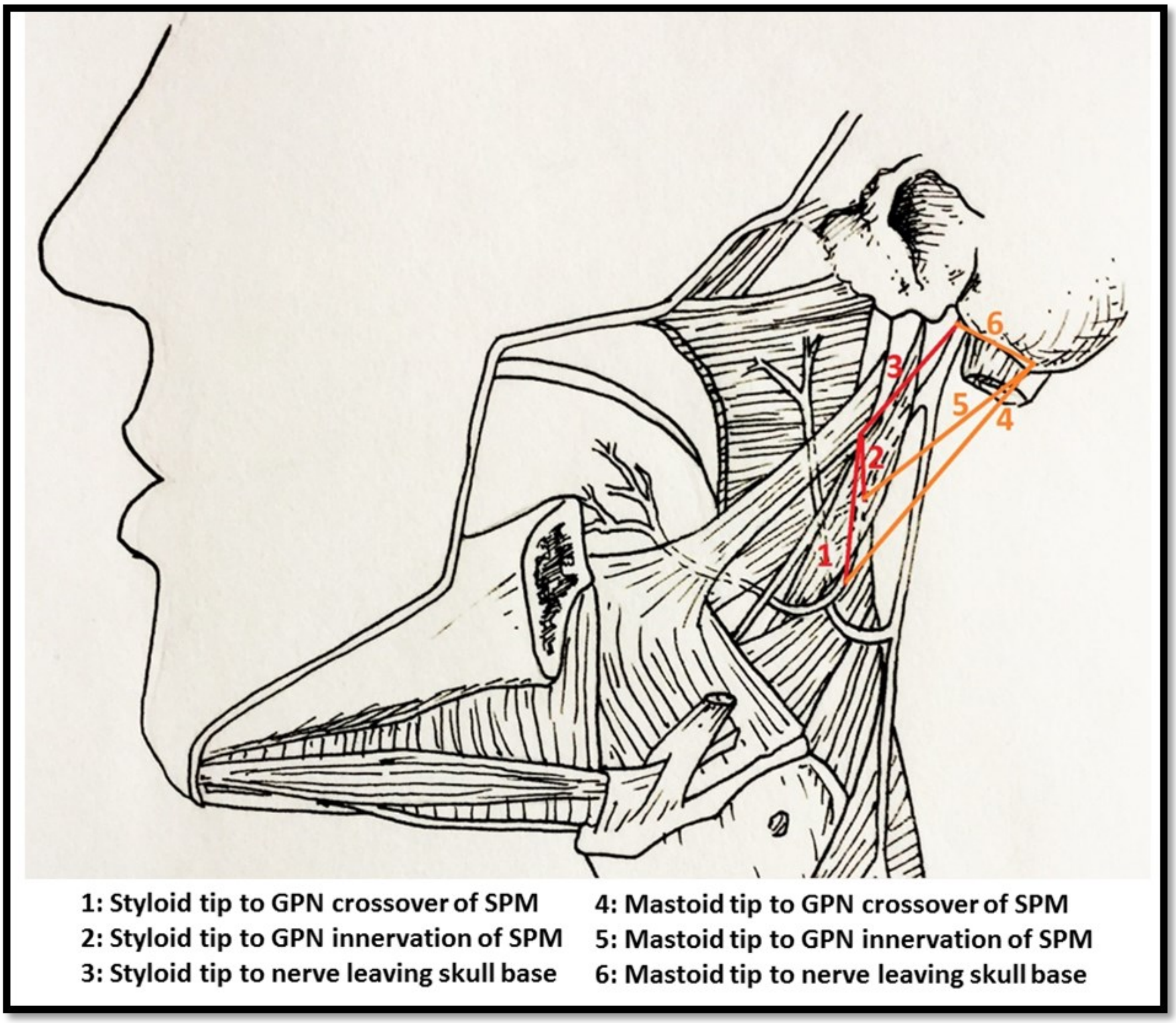

Fig 1. Descriptive map of measurements taken.

Table 1. Average distances between bony landmarks with statistics.

Landmark	Mean Distance (mm)	Standard Deviation (mm)	Maximum (mm)	Minimum (mm)	CV
Mastoid tip to nerve leaving skull base	23.1418	3.7625	31.33	13.69	0.1626
Male Values	23.318	2.4634	27.15	16.95	0.1054
Female Values	22.854	5.0444	31.33	13.69	0.2207
Mastoid tip to innervation of SPM	35.075	7.0665	43.49	8.59	0.2015
Male Values	36.0033	4.1804	43.49	30.57	0.1161
Female Values	33.961	9.6244	40.89	8.59	0.2834
Mastoid tip to nerve crossover of SPM	43.191	8.1967	52.81	12.46	0.1898
Male Values	44.0509	5.4978	52.81	35.29	0.1248
Female Values	42.245	10.6687	48.28	12.46	0.2525
Length of mastoid process	10.5559	2.1969	15.91	6.92	0.2082
Male Values	11.0783	2.3134	15.91	6.92	0.2088
Female Values	9.929	1.9799	12.53	7.22	0.1994
Styloid tip to nerve leaving skull base	22.34	7.52	44.63	14.41	0.3367
Male Values	23.3175	9.5277	44.63	14.41	0.4086
Female Values	21.169	4.2724	30.07	16.05	0.2018
Styloid tip to innervation of SPM	11.5491	8.4436	44.94	3.9	0.7317
Male Values	10.7292	4.6839	17.7	3.9	0.4366
Female Values	12.533	11.7289	44.94	4.54	0.9358
Styloid tip to nerve crossover of SPM	17.86	8.04	50.46	10.13	0.4504
Male Values	15.9191	3.3262	20.4	10.13	0.2089
Female Values	19.997	11.0242	50.46	13.83	0.5513
Length of styloid process	29.4	6.8783	44.83	19.46	0.2339
Male Values	29.6733	8.7829	44.83	19.46	0.296
Female Values	29.077	3.9869	35.06	23.92	0.1371

formed using a mixture of ethanol, glycerin, formaldehyde, and phenol.

Dissections were completed on all heads in the same format by a single dissector. Once the landmarks, which are listed below, were exposed and cleaned, a single pin was placed at each of the landmarks, ensuring accuracy in measurements.

1) Distance from the SPM origin to the proximal innervation along the muscle.
2) Distance between the innervations along the muscle.
3) From the Mastoid Tip to:
   - GPN leaving the skull base.
   - GPN crossing over the SPM.
   - Proximal entrance of the GPN into the SPM.
4) From the Styloid Tip to:
   - GPN leaving the skull base.
   - GPN crossing over the SPM.
   - Proximal entrance of the GPN into the SPM.
5) Length of the styloid process.
6) Length of the mastoid process.
7) Length of the GPN from:
   - Skull base leaving the jugular foramen to the proximal branch of the SPM innervation.
   - Proximal branch of the SPM innervation to the nerve crossover of the SPM.
   - Nerve crossover of the SPM to the entrance into the pharynx between the superior and middle constrictors.

MRI Scans Protocol

To test the viability of using MRI to measure the MP-Length and SP-Length, we acquired a fat-suppressed, 3D FLASH T1 data set using Siemens TIM-Trio 3.0T MRI (Erlangen, Germany) from one subject (TE = 3.69, TR = 9.13, 0.9mm iso, FOV = 256x256, FA=12). Then, using the DICOM viewer Osirix 8.0 (Bernex, Switzerland), we rotated the planes to maximize the visualization of the MP (data not shown), SP, and SPM. In addition, we were able to visualize the GPN to its innervation of the SPM.

Statistical analysis

Microsoft Excel® was used to calculate means, standard deviations, median, standard error, and coefficient of variation (CV). Multiple regression analysis was carried out using Statistical Package

Table 2. Average distances between soft tissue landmarks with statistics .

Landmark	Mean Distance (mm)	Standard Deviation (mm)	Maximum (mm)	Minimum (mm)	CV
SPM origin to GPN innervation	30.0964	6.3856	37.27	16.28	0.2122
Male Values	27.5283	6.7756	35.38	16.28	0.2461
Female Values	33.178	4.4377	37.27	23.17	0.1338
Distance between innervations	5.66	2.4638	12.33	1.75	0.435
Male Values	5.9575	3.0936	12.33	1.75	0.5193
Female Values	5.2711	1.3092	7.01	3.44	0.2484
Nerve length – skull base to innervation	20.89	5.2064	33.5	14.02	0.2492
Male Values	20.1133	6.0602	33.5	14.02	0.3013
Female Values	21.822	4.0732	27.68	15.67	0.1867
Nerve length – innervation to crossover	11.4267	4.0218	19.4	4.27	0.352
Male Values	11.8845	4.9869	19.4	4.27	0.4196
Female Values	10.923	2.7881	15.3	5.82	0.2553
Nerve length – crossover to entrance into pharynx	15.1762	3.5428	24.34	7.05	0.2334
Male Values	16.1827	4.5727	24.34	7.05	0.2826
Female Values	14.069	1.4347	15.9	11.57	0.102
Total nerve length	47.38	4.7388	57.51	39.75	0.1
Male Values	47.8425	4.844	57.51	39.75	0.1012
Female Values	46.814	4.8041	53.8	40.58	0.1026

for the Social Sciences (SPSS). All other statistics and graphing were performed using Graph Pad Prism 5. Welch's t-tests assuming unequal distribution were performed to compare left vs right and male vs female, and significance was determined at a 95% confidence limit. Coefficient of variation was used to assess reliability and consistency. Outliers were identified as being more than two standard deviations outside the mean and excluded from the t-tests. Removal of the outliers had no effect on statistical significance in any t-tests, and those variables were not removed from the results.

RESULTS

Total population results

The mean, standard deviation (SD), maximum, minimum, median, and coefficient of variation (CV) of the distances along the soft tissue landmarks and from the nerve landmarks to the bony landmarks are included in Tables 1 and 2. Additionally, these data were subdivided by gender. These data indicate that all of the measures from the mastoid tip demonstrated less variability than the measures from the styloid process. The total length of the nerve, from the skull base to the entrance into the pharyngeal constrictors had the least amount of variability of the nerve length measurements. Fig. 1 graphically depicts the landmarks measured. Table 3 shows the measurement percentiles as a total population, and subdivided by gender. These percentiles indicate that the given percentage of the measurements made lie within the range listed.

Male versus female measurements

Measurements were divided based on gender, and student's t-tests with Welch's correction were run on each variable. Results illustrate that the distance from the SPM origin to the nerve innervation was significantly higher in females than males, as shown in Fig. 2, but there was no significant difference in any other measurement (data not shown).

Right versus left measurements

Measurements were separated by side of the head and student's t-tests with Welch's correction were run for each variable. No significant difference was found for any of the measures. Data not shown.

Variations of the nerve path

The GPN did wrap around to the lateral side of the SPM, especially in the areas between the stylohyoid and stylopharyngeus muscles, as seen in Fig. 3. Upon dissection, it was noted that 5 of the 22 sides of the heads displayed an interesting variation in the course of the GPN. In these speci-

Table 3. Probabilistic percentiles of the GPN location relative to bony landmarks .

	Styloid Tip to GPN Crossover				Mastoid Tip to GPN Crossover		
	Total	Male	Female		Total	Male	Female
10%	< 12.29 mm	11.65	13.88	**10%**	< 37.75 mm	37.75	39.72
25%	< 14.26 mm	13.78	14.49	**25%**	< 42.18 mm	40.73	43.19
50%	< 16.33 mm	16.33	16.43	**50%**	< 44.44 mm	44.11	45.08
75%	< 18.90 mm	18.70	19.01	**75%**	< 47.12 mm	47.28	47.09
90%	< 20.40 mm	18.92	24.63	**90%**	< 48.28 mm	51.93	48.19
	Styloid Tip to SPM Innervation				**Mastoid Tip to SPM Innervation**		
	Total	**Male**	**Female**		**Total**	**Male**	**Female**
10%	< 5.03 mm	5.03	6.25	**10%**	< 30.65 mm	31.48	27.07
25%	< 6.93 mm	7.50	7.11	**25%**	< 33.55 mm	33.75	33.73
50%	< 9.43 mm	10.28	9.05	**50%**	< 35.36 mm	34.93	37.06
75%	< 12.87 mm	13.63	12.01	**75%**	< 39.04 mm	38.25	39.50
90%	< 17.41 mm	17.41	16.95	**90%**	< 40.87 mm	42.71	40.69
	Styloid Tip to Nerve Leaving the Skull Base				**Mastoid Tip to Nerve Leaving the Skull Base**		
	Total	**Male**	**Female**		**Total**	**Male**	**Female**
10%	< 16.11 mm	14.84	16.61	**10%**	< 19.66 mm	22.00	19.02
25%	< 17.90 mm	17.87	17.96	**25%**	< 21.26 mm	22.93	20.21
50%	< 20.42 mm	19.76	21.46	**50%**	< 23.36 mm	23.71	21.66
75%	< 22.99 mm	24.57	22.99	**75%**	< 25.26 mm	24.41	26.08
90%	< 32.26 mm	36.57	24.76	**90%**	< 27.06 mm	25.31	28.44

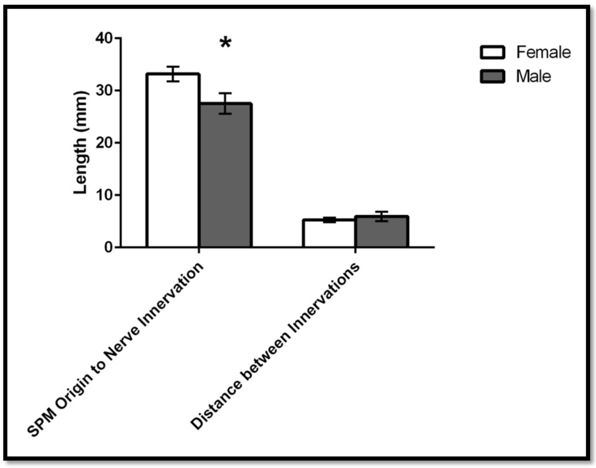

Fig 2. Length from origin of SPM to nerve innervation is longer in females

mens, the nerve exited the jugular foramen and traveled inferiorly along the posterior surface of the SPM, as previously reported (Prades et al., 2014). However, instead of crossing over to the anterolateral side of the SPM, the nerve penetrated the muscle and completed its course to enter into the pharynx, making it impossible to determine where the crossover of the nerve was located, as seen in Fig. 4. For these cadaveric heads, the fibers of the SPM that covered the GPN were resected allowing the location of the nerve crossover to be deter-

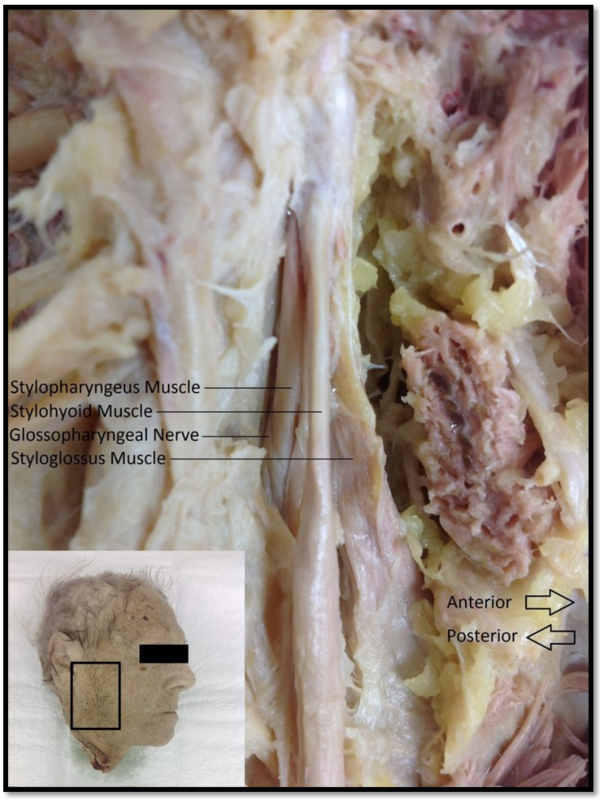

Fig 3. Styloid diaphragm. The styloid diaphragm was exposed, allowing for visibility of the GPN coursing inferiorly in the lateral neck.

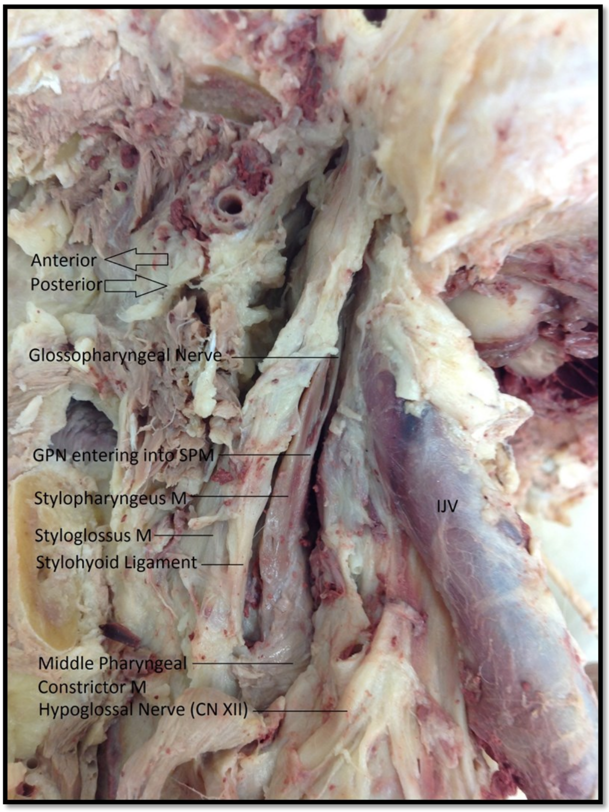

Fig 4. Variation of GPN entering into SPM observed on four specimens

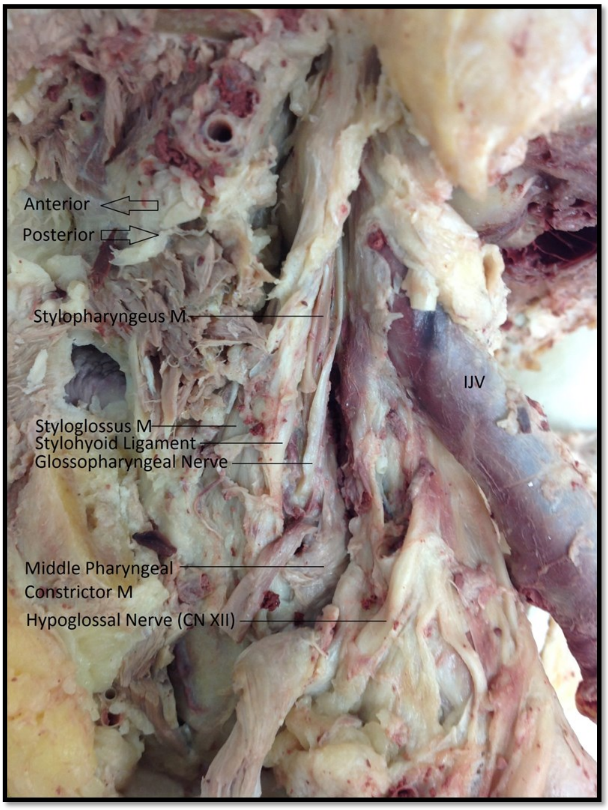

Fig 5. Exposure of GPN inside the SPM variation. Part of the SPM has been resected away to expose the GPN as is courses inferior and anterior inside the SPM.

mined for measurements to be taken, as seen in Fig. 5.

Prediction of nerve location

Multiple regression analysis was performed to construct reliable models in order to predict the location of the GPN as it courses through the lateral neck. Abbreviations below are as follows:

NL_SB_Inn **-** GPN length from skull base to innervation.

SPM_O_NI - SPM length from origin to nerve innervation.

SP_Length **-** Styloid Process Length.

MP_Length **-** Mastoid Process Length.

MT_SMPi **-** Distance from tip of Mastoid Process to the innervation of SPM.

The first model uses the length of the styloid process and the distance from the origin of the SPM to the innervation of the SPM to predict the nerve length from the skull base to the innervation of the SPM [F(2,19) = 7.562, p = 0.004, R^2 = 0.443, R^2 adj = 0.385] (see equation below and Fig. 6).

NL_SB_Inn = 14.075 + 0.605(SPM_O_NI) – 0.387(SP_Length)

The second model incorporates the length of the mastoid process and the length of the styloid process as independent variables to predict the length of the SPM from the origin to innervation [F(2,19) = 6.851, p = .006, R^2 = 0.419, R^2 adj = 0.358] (See equation below and Fig. 6).

SPM_O_NI = 27.477 + 0.548(SP_Length) – 1.279(MP_Length)

Furthermore, a correlation was found between the length of the mastoid process and the distance from the mastoid tip to the innervation of the SPM [F(1,20) = 5.561, p = 0.029, R^2 = 0.218, R^2 adj = 0.178] (See equation below and Fig. 7).

MT_SMPi = 50.912 - 1.500(MP_Length)

Confirmation of GPN pathway

Labeled cardinal plane (axial, coronal, sagittal) images of the MP, SP, and branches of the GPN are visible on T2 MR images (Fig. 8) from IMAOS.com (Montpellier, France; obtained with permission). However, each of the MP, SP, and pharyngeal branch of the GPN course obliquely to each of the cardinal planes. The location of the GPN in relation to the styloid diaphragm was related as posterior and lateral to the SPM (Fig. 8). In addition, we were able to visualize the GPN to its innervation of the SPM as seen in the 3D FLASH T1 images (Fig. 9).

DISCUSSION

The purpose of this study was to identify reliable, consistent landmarks and their distances from the GPN, as well as any differences between landmarks across gender and side of the head. To the best of our knowledge, this is the first study to offer substantial quantitative data suggesting that the mastoid process is a more consistent and reliable landmark than other bony landmarks and to offer

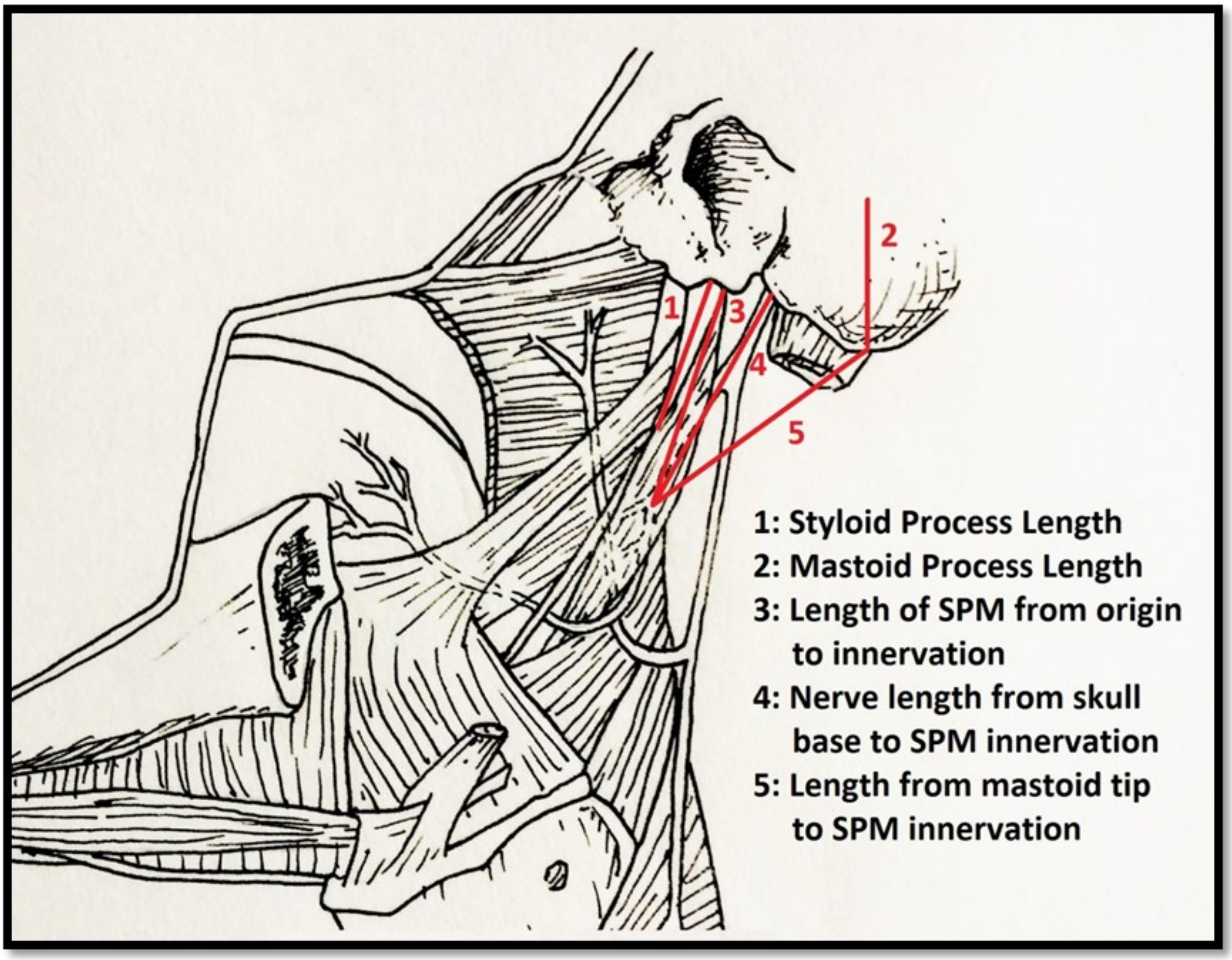

Fig 6. Measurements for multiple regression analysis and statistical model construction for location of the GPN.

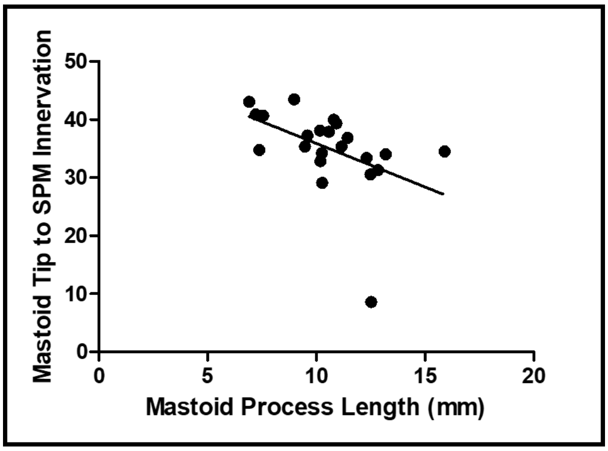

Fig 7. Statistical association between the mastoid process and the length from the mastoid tip to the innervation of the SPM [F(1,20) = 5.561, p = 0.029, R2 = 0.218, R2 adj = 0.178].

reliable models to locate the GPN. Unfortunately, the side of the head and the gender were not reliable markers of GPN location. Future studies could use these variables, and others, such as cranium and head shape, size of cranium and head to possibly identify other variables that can serve as markers of the GPN.

Reliable Landmarks

Previous studies of the GPN have aimed at characterizing the nerve in the jugular foramen (Keles et al., 2009), traveling to the tonsillar bed (Lim et al., 2013), and in relation to the styloid diaphragm (Prades et al., 2014). Other studies have looked at the course of the GPN, and offered general landmarks that could be used, but offer little in the way of quantitative data regarding those landmarks (Goodwin et al., 1993; Ozveren et al., 2003). Table 1 demonstrates that the measurements from the mastoid process, with their low standard deviations, standard errors, and coefficients of variation, are most likely to be consistent across all populations. This establishes the mastoid process as a powerful landmark for surgeons to use in localization and identification of the GPN. Other landmarks, such as the C1 transverse process, were not compared in this study, and future comparisons between these landmarks would be beneficial to elicit which landmark is the most powerful marker.

Substantial variation was noted among styloid process lengths and in measurements originating from the styloid process. The variation of the

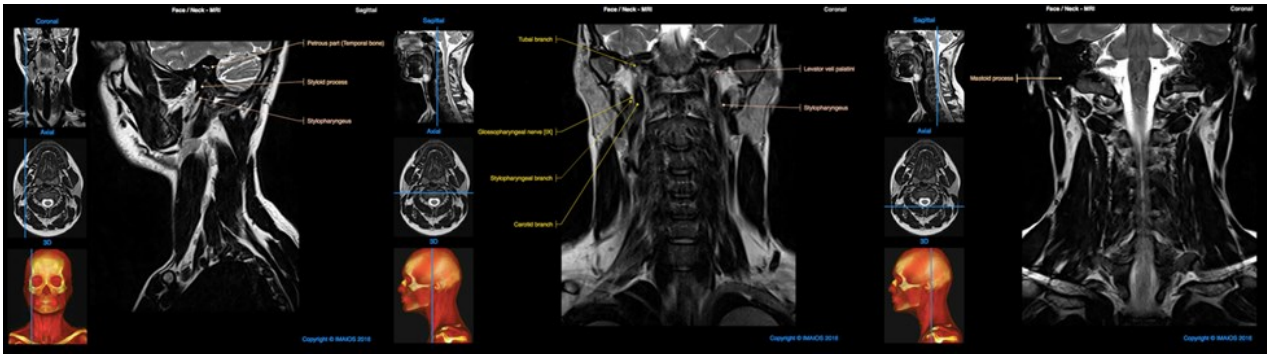

Fig 8. T2 MRI images of the mastoid process, styloid process and glossopharyngeal nerve branches. Images obtained by permission from IMAOS.com (Montpellier, France).

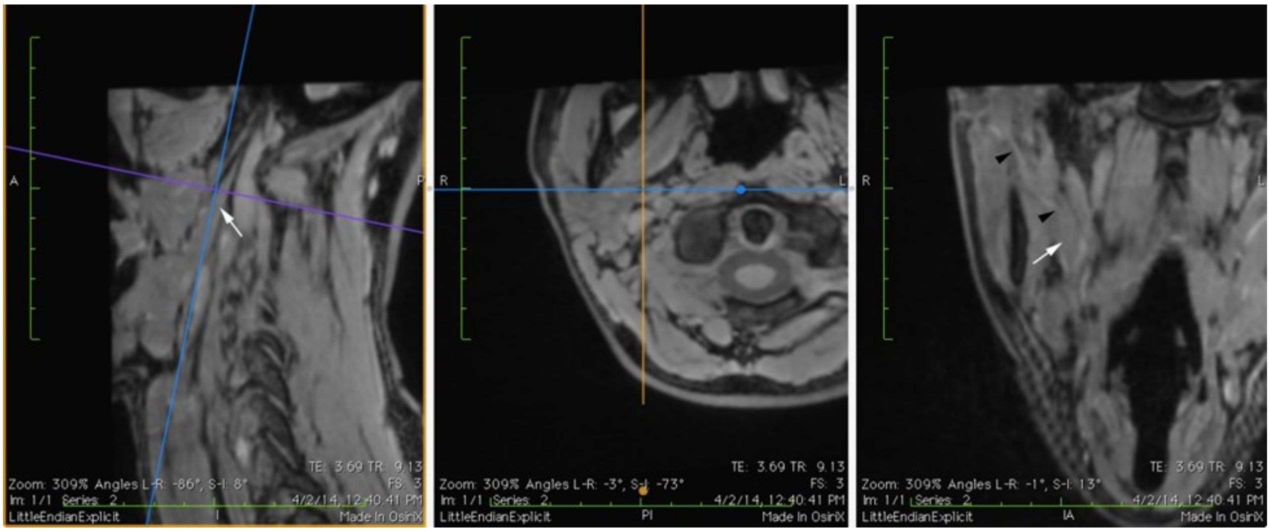

Fig 9. FLASH 3D T1 fat-suppressed MRI images of the styloid process (left and center panels under the axes), stylopharyngeus muscle (white arrow) and glossopharyngeal nerve and its innervation point of the muscle (black arrowheads). The blue axis on the left panel corresponds to the image in the left panel. The purple axis in the left panel corresponds to the image in the center panel.

measurements originating from the styloid process is likely a result of the variance of the length of the styloid process. Variance of the styloid process is possibly due to a calcification of the stylohyoid ligament, increasing measured length of the process and confounding other measurements. When calcification of this ligament extends too far, it can compress other soft tissue structures causing pain and damage, and is known as Eagle Syndrome (Ferreira et al., 2014). Thus, while the styloid process and tip are very close to the GPN and the styloid diaphragm, it is a weak landmark due to the variation of length.

Logistical map of the GPN

With the information gathered from this study, a rudimentary percentile map was created to aid surgeons in their quest to correctly identify the GPN. The measurements from the bony landmarks and along soft tissue landmarks were useful in the creation of the map; however, further studies are needed to complete it. Some of these studies might include measurements from the bony landmarks to the nerve at the same level, or along a sagittal plane. Removal of extraneous tissue not innervated by, or associated with the nerve, followed by 3D scanning would help to create a working 3D model that would aid not only surgeons, but also medical and anatomical students seeking clarification of the nerve path.

The results of this study were consistent with past studies as the GPN does wrap around to the lateral side of the SPM (Institute NC, 2013; Oncology Asoc., 2014), especially in the areas between the stylohyoid and stylopharyngeus muscles, as seen in Fig. 3.

The multiple regression analyses were used to create equations with which surgeons could correctly identify the location of the innervation of the SPM by the GPN. Using the measurements of the styloid process length, mastoid process length, distance from the mastoid tip to the SPM innervation, nerve length from skull base to SPM innervation, and SPM length from its origin to the innervation by GPN, three equations were formed as predictive models for the location of the GPN innervation of the SPM:

$$SPM\_O\_NI = 27.477 + 0.548(SP\_Length) - 1.279(MP\_Length)$$

$$NL\_SB\_Inn = 14.075 + 0.605(SPM\_O\_NI) - 0.387(SP\_Length)$$

$$MT\_SPMi = 50.912 - 1.500(MP\_Length)$$

Measurements such as MP_Length and SP_Length are easily seen on radiographs, such as a CT scan. Identification of where the GPN leaves the skull base has previously been identified as the anteromedial potion of the jugular foramen (Keles et al., 2009), making identification of the NL_SB_Inn possible with the models produced in this study.

MRI tracing of GPN

Visualization of the GPN to its innervation of the SPM was clearly visible in the 3D FLASH T1 images. 3D T2 images were not acquired, since the time of acquisition of a 3D image was excessive. Future studies will investigate the optimization of acquiring 3D T1 and T2 images for the purposes of pre-surgical planning.

Summary. In this study we showed that the mastoid process is a more consistent, and thus more reliable, bony landmark than the styloid process in predicting the location of the GPN. Furthermore, distances between different landmarks along the GPN have been characterized, and models have been created to help identify location of those landmarks.

ACKNOWLEDGEMENTS

The authors acknowledge the help of Charles Madden in providing the illustrations accompanying this work. The authors also wish to thank individuals who donate their bodies and tissues for the advancement of education and research.

REFERENCES

BOUDREAUX BA, ROSENTHAL EL, MAGNUSON JS, NEWMAN JR, DESMOND RA, CLEMONS L, CARROLL WR (2009) Robot-assisted surgery for upper aerodigestive tract neoplasms. *Arch Otolaryngol Head Neck Surg*, 135(4): 397-401.

COGNETTI DM, WEBER RS, LAI SY (2008) Head and neck cancer: an evolving treatment paradigm. *Cancer*, 113(7 Suppl): 1911-1932.

FERREIRA PC, MENDANHA M, FRADA T, CARVALHO J, SILVA A, AMARANTE J (2014) Eagle syndrome. *J Craniofac Surg*, 25(1): e84-86.

GOODWIN WJ, JR, ARNOLD D, WACHHOLZ J (1993) Surgical anatomy of the glossopharyngeal nerve. *Laryngoscope*, 103(11 Pt 1): 1302-1304.

GREYLING LM, GLANVILL R, BOON JM, SCHABORT D, MEIRING JH, PRETORIUS JP, VAN SCHOOR A (2007) Bony landmarks as an aid for intraoperative facial nerve identification. *Clin Anat*, 20(7): 739-744.

INSTITUTE NC. (2013) Head and Neck Cancers. Available from: http://www.cancer.gov/cancertopics/types/head-and-neck/head-neck-fact-sheet.

KELES B, SEMAAN MT, FAYAD JN (2009) The medial wall of the jugular foramen: a temporal bone anatomic study. *Otolaryngol Head Neck Surg*, 141(3): 401-407.

KITAGAWA J, SHINGAI T, TAKAHASHI Y, YAMADA Y (2002) Pharyngeal branch of the glossopharyngeal nerve plays a major role in reflex swallowing from the pharynx. *Am J Physiol Regul Integr Comp Physiol*, 282 (5): R1342-1347.

LIM CM, MEHTA V, CHAI R, PINHEIRO CN, RATH T, SNYDERMAN C, DUVVURI U (2013) Transoral anatomy of the tonsillar fossa and lateral pharyngeal wall: anatomic dissection with radiographic and clinical correlation. *Laryngoscope*, 123(12): 3021-3025.

NGUYEN NP, MOLTZ CC, FRANK C, KARLSSON U, SMITH HJ, NGUYEN PD, VOS P, NGUYEN LM, ROSE S, DUTTA S, SALLAH S (2005) Severity and duration of chronic dysphagia following treatment for head and neck cancer. *Anticancer Res*, 25(4): 2929-2934.

ONCOLOGY ASOC. (2014) Head and Neck Cancer: Treatment Options cancer.net. Available from: http://www.cancer.net/cancer-types/head-and-neck-cancer/treatment-options.

OZVEREN MF, TURE U, OZEK MM, PAMIR MN (2003) Anatomic landmarks of the glossopharyngeal nerve: a microsurgical anatomic study. *Neurosurgery*, 52(6): 1400-1410; discussion 10.

PATHER N, OSMAN M (2006) Landmarks of the facial nerve: implications for parotidectomy. *Surg Radiol Anat*, 28(2): 170-175.

PEREIRA JA, MERI A, POTAU JM, PRATS-GALINO A, SANCHO JJ, SITGES-SERRA A (2004) A simple method for safe identification of the facial nerve using palpable landmarks. *Arch Surg*, 139(7): 745-747; discussion 8.

PIKUS L, LEVINE MS, YANG YX, RUBESIN SE, KATZKA DA, LAUFER I, GEFTER WB (2003) Videofluoroscopic studies of swallowing dysfunction and the relative risk of pneumonia. *AJR Am J Roentgenol*, 180 (6): 1613-1616.

PRADES JM, GAVID M, ASANAU A, TIMOSHENKO AP, RICHARD C, MARTIN CH (2014) Surgical anatomy of the styloid muscles and the extracranial glossopharyngeal nerve. *Surg Radiol Anat*, 36(2): 141-146.

SAKAMOTO Y (2009) Classification of pharyngeal muscles based on innervations from glossopharyngeal and vagus nerves in human. *Surg Radiol Anat*, 31(10): 755 -761.

SANDERSON RJ, IRONSIDE JA (2002) Squamous cell carcinomas of the head and neck. *BMJ*, 325(7368): 822-827.

SURGERY AAOO-HAN (2014) 50 Facts about Oral, Head and Neck Cancer. Available from: http://www.entnet.org/?q=node/1501.